Short Glass Fiber Reinforced Radiation Crosslinked Shape Memory SBS/LLDPE Blends

Wang Yongkun, Zhu Guangming, Tang Yusheng, Liu Tingting, Xie Jianqiang, Ren Fang
Department of Applied Chemistry, Northwestern Polytechnical University, Xi'an 710129, China
Correspondence to: Z. Guangming (E-mail: gmzhu@nwpu.edu.cn)

ABSTRACT: The poly(styrene-*b*-butadiene-*b*-styrene) triblock copolymer (SBS) and linear low density polyethylene(LLDPE) were blended and irradiated by γ-rays to prepare shape memory polymer(SMP). Various amounts of short glass fiber (SGF) were filled into SMP to form a novel shape memory SGF/SBS/LLDPE composite. The effect of SGF on the shape memory SGF/SBS/LLDPE composite was studied in terms of mechanical, dynamic mechanical analysis (DMA), differential scanning calorimetry (DSC) and shape memory effects. It is found that the SGF act as reinforcing fillers and significantly augment the glassy and rubbery stated moduli, tensile strength and shape memory properties. When SGF content is <2.0 wt %, full recovery can be observed after only several minutes at different temperatures and shape recovery speed reduces as the SGF content increases. The shape recovery time decreases as the temperature of the shape memory test increases and the shape recovery rate decreases with increment of cycle times. © 2014 Wiley Periodicals, Inc. J. Appl. Polym. Sci. **2014**, *131*, 40691.

INTRODUCTION

Shape memory polymers (SMPs) are those that have the capability of rapidly changing their shapes from a temporary shape to a permanent shape upon application of appropriate external stimulus such as heat, light, electric field, magnetic field, PH, specific ions, and enzyme.[1-8] Among them, thermally activated SMPs are the most common. The basic mechanism of shape recovery can be attributed to "shrinkage" of oriented, extended chains triggered, for example, by melting or glass transition.[4] Over shape memory metallic alloys and shape memory ceramics, SMPs have the advantages of light weight, low cost, good processability, high shape recoverability, and tailorable switch temperature. Thus, SMPs provide greatly values for a wide range of applications, including smart textiles and apparels, heat shrinkable packaging, intelligent biomedical materials and self-deployable structures in spacecrafts.[8-12]

Nevertheless, there are some scientific and technological barriers which prevent widespread applications and development of SMPs compared with shape memory metallic alloys and shape memory ceramics. For instance, lower mechanical strength and shape recovery stress. Usually, the recovery stress of SMPs is 1–3 MPa compared to 0.5–1 GPa for shape memory alloys.[4,13] Therefore, much effort has been made to overcome these problems. To date, one of the immediate methods is using high modulus inorganic or organic fillers to reinforce pristine SMPs, and shape memory composites are therefore developed. However, it has been observed that there is a trade-off between enhancement of modulus and reduction of shape memory behavior. Generally, fillers exert negative impact on recoverable strain due to their sizes, and substantially higher stiffness compared to the matrix polymer. In some cases, they even disturb the polymer networks responsible for shape memory functions, especially at high loading levels.[14-16] Consequently, there are numerous efforts have been made to strike a balance between the recovery stress and recovery strain with the use of fillers. Luo et al.[17] filled shape memory polyurethane with cellulose nano-whiskers. They found that the modulus of composites was higher than the pure polyurethane. And the results also indicated that the shape fixity ratio was increased with the increment of the content of nano-whiskers. However, the shape recovery ratio rapidly decreased with the increasing of the content of nano-whiskers, and the shape recovery ratio was only about 20% when the content of nano-whiskers up to 23 wt %. Auad et al.[18] investigated the shape memory behavior of nano-cellulose reinforced polyurethanes. The results showed that the modulus of shape memory polymers improved 53% and creep deformation decreased about 36% by adding 1 wt % nano-cellulose. Meanwhile, this improvement did not have substantial effects on the shape memory behavior.

However, to our knowledge, there are only a few literatures investigated shape memory behavior of radiation crosslinked
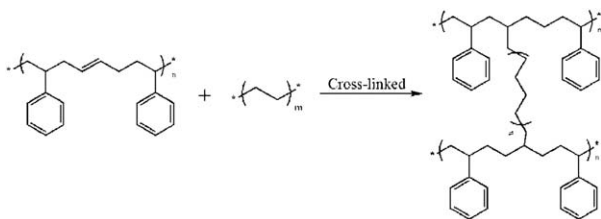
Scheme 1. Crosslinked SBS/LLDPE blends.

poly(styrene-*b*-butadiene-*b*-styrene) triblock copolymer(SBS)/ linear low density polyethylene (LLDPE) blends reinforced by short glass fiber(SGF). This study aims to develop a type of shape memory composites with good comprehensive performance to meet the needs of the engineering application. And a series of shape memory SGF/SBS/LLDPE composites were prepared with various weight fractions of SGF. The thermomechanical properties and shape memory behaviors of the developed composites were fully characterized and systematically investigated.

EXPERIMENTAL

Materials
SBS (PS: PB = 30/70) was purchased from Balin Petrolem Chemical Corporation, Sinopec Group, China. LLDPE was produced by Tianjin Petro-Chemical, China. The SGF (437H, Taishan glass fiber) ∼3 mm in length and 14 μm in diameter was obtained by continuous cutting of E-glass fiber. These materials were used without further purification.

Preparation and Sample Irradiation
SBS, LLDPE, and SGF were blended in a Banbury mixer (PLE 651, Brabender, Germany) at 130°C for 10 min. After blending, the samples were compressed into plates in a hot press at 160°C with the pressure of 10 MPa.

The specimens were irradiated at 50, 100, 150, 200, and 250 kGy by [60]Co γ-rays under vacuum (10^{-3} torr) at 20–30°C at a dose rate of 1 Gy s^{-1}. The dose range of 50 to 250 kGy was selected because numerous previous studies had successfully demonstrated electron beam crosslinking of various polymer systems within this dose range.[19,20] In the SBS/LLDPE blends, the crosslinking between SBS and LLDPE can form an interpenetrating of hard and soft phase condensed state structure SMP material (Scheme 1). After the curing process, the thickness of all the developed composites were ∼2 mm. Shape memory SGF/SBS/ LLDPE composites with SGF weight fractions of 0.5, 1.0, 1.5, 2, and 2.5 wt % were fabricated in this way. For comparison, a pure SMP specimen was cured under the same conditions. The optimized radiation dose was chosen from aforementioned radiation dose, and then was used to irradiate the SGF/SBS/LLDPE composites.

Methods
FTIR. Structural changes in the shape memory SGF/SBS/LDPE composites were investigated using an FTIR spectrometer (Nicolet iS10, Thermo Fisher Scientific, Waltham, MA) from 4000 to 500 cm^{-1}.

Sol/Gel Analysis. To estimate the degree of cross-linking of the SBS/LLDPE blends, the sol/gel analysis was performed on samples. Triplicate samples with masses of about 50 mg were

cut from the samples, and copper net was used to wrap samples then weighing it. Benzene was chosen as the solvent, and then the sample–solvent mixtures were heated to 120°C for 72 h and determined by the method of solvent extraction. The swollen gels were then removed from the vials and washed with acetone to remove residual solvent. At last, the samples were dried in oven for 6 h, and the dried samples were re-massed, gel fractions were calculated according to eq. (1)

$$g = (m_2 - m_1)/m_0 \times 100\% \qquad (1)$$

where g is gel fraction, m_0 is initial weight, m_1 is copper net, m_2 is gel and copper net weight.

Mechanical Properties. Tensile tests at room temperature were carried out on a tensile test instrument (SANS PowerTest v3.0, Shenzhen SANS Material Test Instrument, China) according to ASTM D412. The strain rate was 100 mm min^{-1}. The tensile strength and elongation at break were recorded during the experiments.

Differential Scanning Calorimetry (DSC). The melting temperatures (T_m) of the samples were determined with differential scanning calorimetry (DSC, Pyris 1, Perkin Elmer, USA). Samples of about 5.0 mg were heated from 0 to 130°C at a constant rate of 10°C min^{-1} and then passed through a cooling cycle with the same rate, and T_ms were determined by this step. The differences among the T_ms of the different SGF content composites were determined from the DSC.

Dynamic Mechanical Analysis (DMA). DMA samples were cut to dimensions of 2 × 12 × 30 mm^3 and the edges of the samples were wet sanded with 600 grit sandpapers. DMA was performed in single cantilever clamping fixture and run on a TA Q800. A small dynamic load at 1 Hz was applied to a platen and the temperature was ramped from −10 to 150°C at a rate of 3°C min^{-1}. The amplitude was set to be 10 μm.

Scanning Electron Microscopy (SEM). SEM (INCA X-ACT) was used to observe the cross-sectional morphology of the composites.

Shape Memory Behavior Test. Rectangular specimens (100 mm × 10 mm × 2 mm) were used to evaluate the shape memory property of the SGF/SBS/LLDPE composites. The shape memory model was shown in Figure 1, and the shape recovery test was performed according to the following steps: (i) the specimens were heated up to the deformation temperatures in an oven and held for 10 min; (ii) the specimens were bent into "U" shape under constant force; (iii) the "U" shaped specimens were then quickly removed from the oven and dipped into a cold water bath with a constant external force; (iv) heating up the specimens to deformation temperature, the shape recovery process was observed and the shape recovery angles were recorded. When the specimens did not change, the recovery time was recorded. For each amount of short glass fiber, five specimens were measured to achieve the average recovery time. The deformation recovery speed corresponding temperature is defined as θ_i/t, and the deformation recovery rate is defined as $(\theta_i - \theta_f)/\theta_i \times 100\%$.

RESULTS AND DISCUSSION

FTIR Analysis
The FTIR spectra of SGF, uncross-linked SBS/LLDPE blend and SGF/SBS/LDPE composites are presented in Figure 2. As can be seen from Figure 2, the most characteristic features in the FTIP
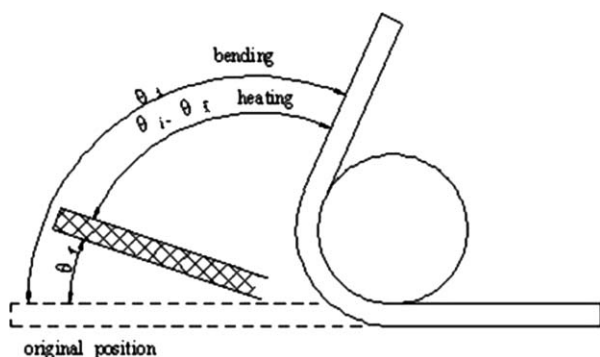
Figure 1. Shape memory model.

Figure 3. Gel content of radiation crosslinked SBS/LLDPE blends.

spectrum of SGF and SBS/LLDPE blends are the adsorption bands corresponding to Si—OH at 943 cm^{-1} and the C═C stretching at 1621 cm^{-1}. However, it can be found that the adsorption band of C═C in the FTIP spectrum of SGF/SBS/LDPE composite disappears, which is attributed to the effect of radiation crosslinking on the C═C. Furthermore, the additional of adsorption band of Si—OH increases in the FTIP spectrum of SGF/SBS/LLDPE composite, which indicates that the SGF has been filled in the SMP. Therefore, the radiation cross-linked SBS/LLDPE blends reinforced with SGF were successfully prepared.

Gel Content
To choose the appropriate radiation dose for SGF/SBS/LLDPE composites, we should first investigate the crosslinking degree of the SBS/LLDPE blends and study the shape memory effect of the blends. In this work, the radiation crosslinking is radical cross-linking. Because two γ-rays are launched during the ^{60}Co decaying process, the energies of which are 1.173 and 1.332 MeV, respectively. These high energy γ-rays can open the chemical bonds in the polymer chain segment to produce free radicals to initiate free radical crosslinking reaction. Therefore, the cross-linking network structure can be formed in the SBS/LLDPE blends. Figure 3 shows the gel content of SBS/LLDPE blends
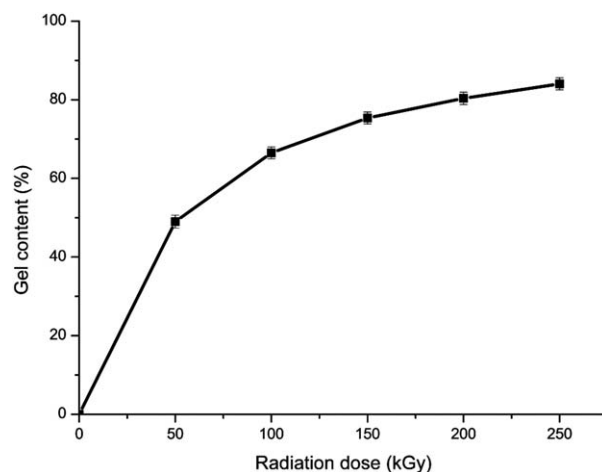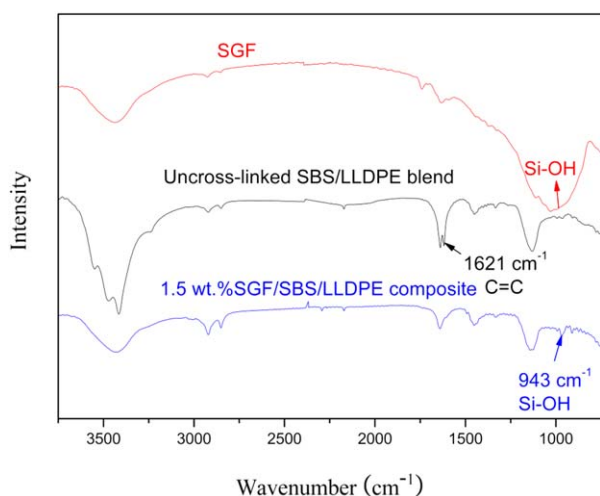

Figure 2. FTIR spectra of SGF, SBS/LDPE blend, and SGF/SBS/LDPE composites. [Color figure can be viewed in the online issue, which is available at wileyonlinelibrary.com.]

versus radiation dose. As the curves indicate, the gel contents increase with the absorbed dose increasing, and the curves then gradually level off after 200 kGy. This phenomenon is attributed to that the free radical increase with the increment of radiation dose, and more cross-linking network structure can be formed. However, when the radiation dose >200 kGy, the gel content is convergence. Similar result can also be found in Ref. 21.

The results of shape memory tests of the SBS/LDPE blend indicate that the gel content of radiation crosslinked SBS/LLDPE blend is 66.5% as the radiation dose is 100 kGy, and shape recovery ratio and shape fixity ratio are nearly 100% for the blends. Thus, the radiation dose chosen for the SGF/SBS/LLDPE composites is 100 kGy, and SGF content has little effect on the gel content of SGF/SBS/LLDPE. Therefore, the cross-linking degree of the SGF/SBS/LLDPE composites is 66.5%.

DSC
To study the shape memory performance of SGF/SBS/LLDPE composites, we should first ascertain the shape memory transition temperatures due to the shape recovery temperatures are chosen based on them. In this work, the shape memory transition temperatures of SGF/SBS/LLDPE composites are routinely determined by DSC, and the shape memory transition temperature as a function of the contents of SGF is shown in Figure 4. The endothermic peaks correspond to the melting temperatures, which are the shape recovery temperatures of composites. Figure 4 illustrates that the shape recovery temperatures of the composite are all about 110°C and unchanged as the content of SGF increase in the composites. This indicates that SGF has no significant effect on T_ms of the composites. However, it can be found that the T_ms of the composites are lower than the pure SMP. This is attributed to that relative motion of macromolecule segments is the primary mechanism of the shape memory effect in the SMPs. Note that the total amount SMP segments per unit in the composite is less than that of pure SMP matrix. Additionally, the thermal conductivity of the SGF, SBS and LDPE is about 1.46, 0.16, and 0.33, respectively. Thus, the SGF filler has a positive effect in increasing thermal conductive of composites and thermal behavior of segments is promoted by
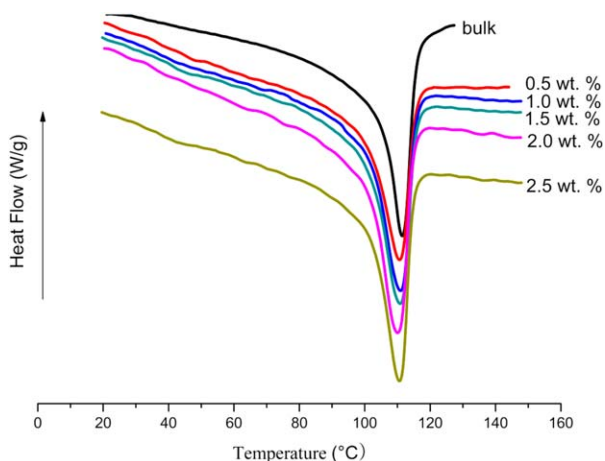
Figure 4. DSC plots of SGF/SBS/LLDPE samples. [Color figure can be viewed in the online issue, which is available at wileyonlinelibrary.com.]

the SGF. Therefore, the T_ms of SGF/SBS/LLDPE composites shift to lower value.

DMA

Usually, a good shape memory composite should have a large change of storage modulus (E') below and above shape memory transition temperature. Figure 5 shows the storage moduli of the SGF/SBS/LLDPE composites below shape memory transition temperature approximately two orders lager than that above shape memory transition temperature, which means that the SGF/SBS/LLDPE composites meet the above requirements. As shown in Figure 5, the storage moduli of all samples decrease slowly along with temperatures increasing, and then descend abruptly when the temperature rise to about 110°C, which is attributed to the melting of the semicrystalline SBS/LDPE matrix. Similar results can be also found in Ref. 12.

Meanwhile, the glassy modulus is closely related to the shape fixity as the deformed shape is fixed upon cooling to glassy state, while the rubbery modulus related to shape recovery as the original shape is recovered in rubbery state. Figure 5 shows
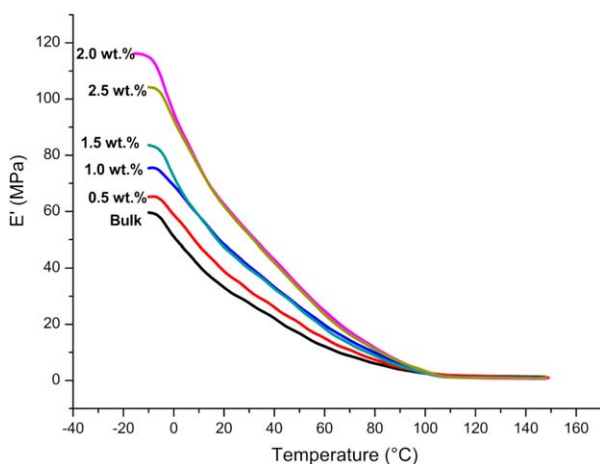

Figure 5. Dynamic mechanical properties of the SGF/SBS/LLDPE composites. [Color figure can be viewed in the online issue, which is available at wileyonlinelibrary.com.]
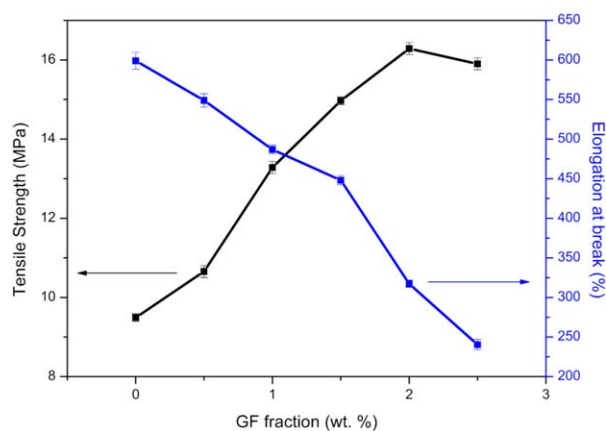

Figure 6. Mechanical property of the SGF/SBS/LLDPE composites. [Color figure can be viewed in the online issue, which is available at wileyonlinelibrary.com.]

that the storage moduli increase as the SGF contents increase but decrease slightly when the SGF content increases to 2.5 wt %. Normally, the storage moduli of specimens will increase by adding glass fiber reinforcement. However, the dispersion of SGF in the SBS/LLDPE blends will be uneven when the SGF content increases to certain amount. The clustering of the SGF will exist in the SBS/LLDPE blends, which prevents each fiber acting independently and contributing to load sharing. In the meantime, it is noted that high SGF content results in void formation. And the void between the matrix and SGF may lead to the load bearing capacity of composites decreasing. Therefore, the storage moduli of composites increase with the increment of SGF but decrease slightly when the SGF content rises to 2.5 wt %.

Mechanical Properties

The tensile property is one of the most important indicators to reveal the mechanical property of SGF/SBS/LLDPE composites. And the relationship between tensile strength and SGF content is illustrated in Figure 6, where each sample is characterized by tensile tests at room temperature. It is seen that the tensile strength of SGF/SBS/LLDPE composites increases with the increment of SGF but decreases when the SGF content increases to 2.5 wt %, and the bulk specimen without SGF has a tensile strength of about 9.5 MPa. Considering the SGF is the reinforcement, the tensile strength of the composites will increase. However, the effect of SGF will be offset by the uneven dispersion of fiber reinforcement. Moreover, higher fiber content leads to form more voids, which will results in micro crack formation under loading, reducing the tensile strength.

The other most important mechanical property of the SMP is the elongation at break. In Figure 6, we present the relationship between Elongation at break and SGF content. It is of significance that the elongation at break of all specimens decreases with the content of SGF increasing. This indicates that the toughness of the composites decreases with the SGF content increasing. And the elongation at break of bulk specimen without SGF reinforcement is about 598.95%, whereas, with 2.5 wt %
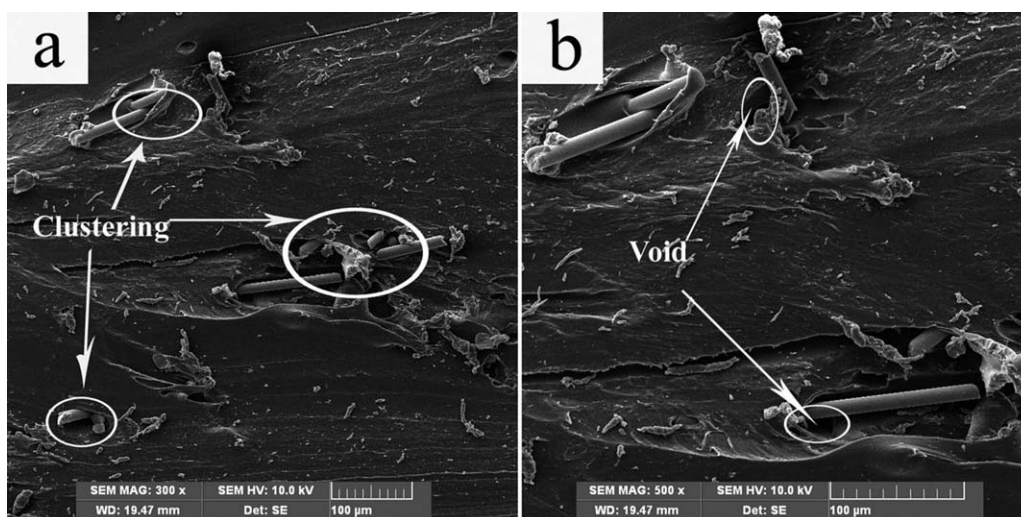
Figure 7. SEM of the specimen with 2.5 wt % SGF.

SGF reinforcement, the elongation at break decreases by about 59.87% than the neat matrix.

To illustrate the mechanical properties of the composites with 2.5 wt % SGF, we observed the microstructures of the specimen. Figure 7 shows the SEM of the specimen with 2.5 wt % SGF at different magnification. Figure 7(a) reveals that the uneven distribution and clustering of the SGF in the matrix. Figure 7(b) illustrates the voids between SGF and matrix. Because of the two factors mentioned above, the mechanical properties of the composites decrease slightly when the SGF content rises to 2.5 wt %.

Shape Memory Behavior Analysis

The shape memory effect of specimen with 0.5 wt % SGF is shown in Figure 8. Stating form the original shape, the specimen is deformed into "U" shape in the oven. Upon cooling under load, the deformed temporary shape is fixed. Then placing the specimen in the 110°C oven, full recovery could be observed after only 160 s.

Figure 9 illustrates the relationship between the recovering angle and recovering time of the bulk, 0.5, 1.0, 1.5, and 2.0 wt %. According to the results, full recovery can be observed after only several minutes at $T_m - 10°C$, T_m, $T_m + 10°C$, and $T_m + 20°C$.
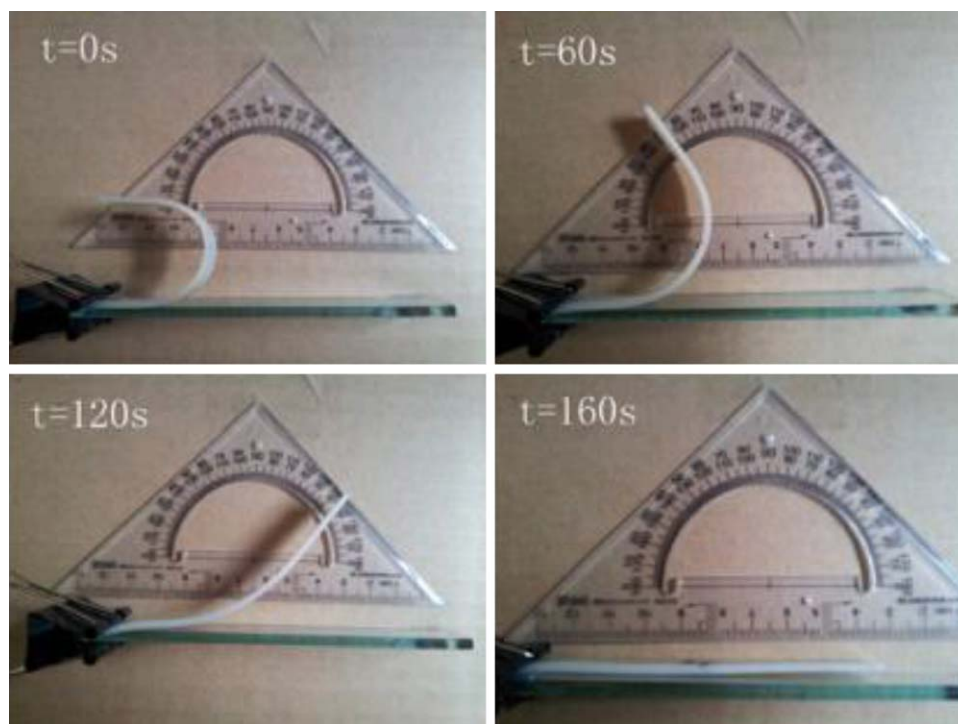

Figure 8. Shape memory effect of composite with 0.5 wt % SGF at 110°C. [Color figure can be viewed in the online issue, which is available at wiley-onlinelibrary.com.]
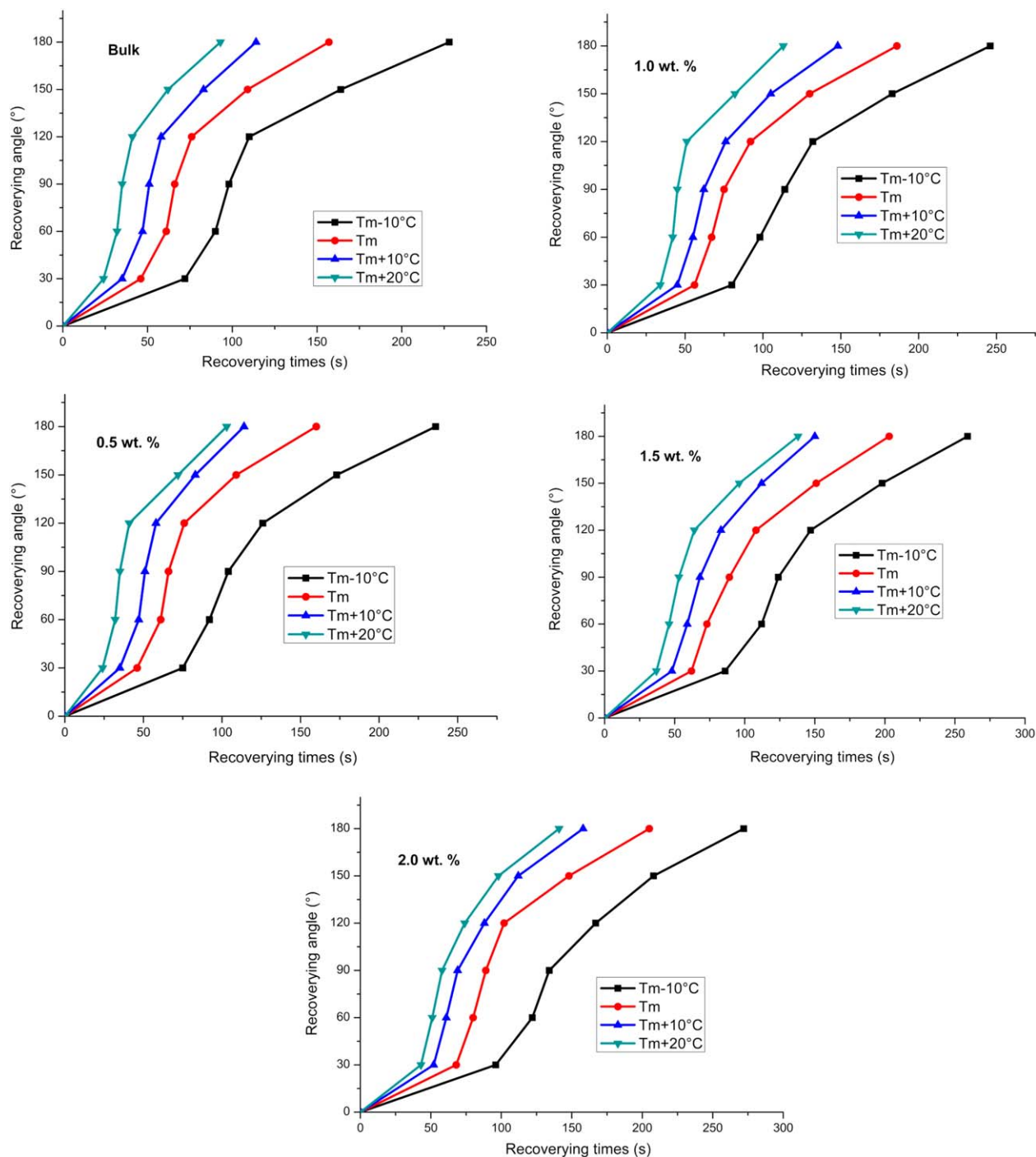
Figure 9. Relationship between recovering angle and recovering time of SGF/SBS/LLDPE composites at different temperatures. [Color figure can be viewed in the online issue, which is available at wileyonlinelibrary.com.]

Therefore, all of the shape recovery ratio of the bulk, 0.5, 1.0, 1.5, and 2.0 wt % specimens is almost 100%. These results demonstrate that the SGF/SBS/LLDPE composites have excellent shape memory performances. Moreover, SGF have not significant effect on the shape memory properties of the developed composites when SGF content between 0.5 and 2.0 wt %, while the shape recovery time slightly increases with the increment of SGF content as the stiffness of the composites increases with the SGF

content increasing. For the same specimen, completing shape recovery at higher temperature costs less time, which is attributed to an increase in macromolecular segment movement. Meantime, as shown in Figure 9, the slope of the curve is generally larger from 30° to 120°. This indicates that the shape recovery rate is high. However, the specimens have a relative low recovery rate at the initial and final stages. At the initial stage, the release of the stored strain energy is followed by heavy friction among
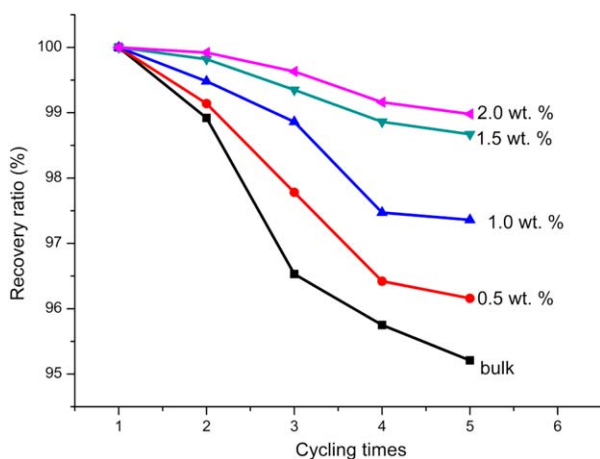
Figure 10. Effects of cycling times on recovery ratio of SGF/SBS/LLDPE composites. [Color figure can be viewed in the online issue, which is available at wileyonlinelibrary.com.]

segments, which would cause decreased recovery rate. When the stored strain energy is released largely at the anterior stage; the recovery rate becomes slow at the final stage. The 2.5 wt % specimen is not used as a shape memory material because it cannot fully recovery to initial.

Figure 10 shows the effect of cycling times on recovery ratio of SGF/SBS/LLDPE composite. It can be found that the shape recovery ratio of composites decreases slightly with increasing cycling times. This phenomenon is attributed to the accumulation of plastic deformations in the composites, which inevitably occurs during the recovery process. In addition, the shape recovery ratio slowly decreases with the increment of the SGF content because an increase in SGF content leads to an increase in stiffness of the materials, resulting in the reduction of plastic deformation.

CONCLUSION

Shape memory SBS/LLDPE composites incorporated with different amounts of SGF were fabricated. The tensile strength of the composites increases with the increment of SGF content but decreases slightly when SGF content rises to 2.5 wt %. The filled SGF causes no change in the shape memory transition temperatures of the composites. When the SGF content is <2.5 wt %, the shape memory SGF/SBS/LLDPE composites show excellent shape memory properties, and full recovery can be observed after only several minutes at different temperatures. The shape recovery time and recovery ratio slightly increase with the increment of SGF content. However, the shape recovery ratio decreases with cycling times increasing.

REFERENCES

1. Sun, L.; Huang, W. M.; Ding, Z.; Zhao, Y.; Wang, C. C.; Purnawali, H.; Tang, C. *Mater. Des.* **2012**, *33*, 577.
2. Meng, Q. H.; Hu, J. L. *Compos. A Appl. Sci. Manufact.* **2009**, *40*, 1661.
3. Zhang, Q.; Yang, Q. S. *J. Appl. Polym. Sci.* **2012**, *123*, 1502.
4. Gunes, I. S.; Cao, F.; Jana, S. C. *Polymer* **2008**, *49*, 2223.
5. Liu, Y. J.; Lv, H. B.; Lan, X.; Leng, J. S.; Du, S. Y. *Compos. Sci. Technol.* **2009**, *69*, 2064.
6. Zhang, H.; Wang, H. T.; Zhong, W.; Du, Q. G. *Polymer* **2009**, *50*, 1596.
7. Wang, W.; Wang, X. Z.; Cheng, F. T.; Yu, Y. L.; Zhu, Y. T. *Prog. Chem.* **2011**, *23*, 1165.
8. Fulcher, J. T.; Karaca, H. E.; Tandon, G. P.; Lu, Y. C. *J. Appl. Polym. Sci.* **2013**, *129*, 1096.
9. Yang, D.; Huang, W.; He, X. H.; Xie, M. R. *Polym. Int.* **2012**, *61*, 38.
10. Voit, W.; Ware, T.; Gall, K. *Polymer* **2010**, *51*, 3551.
11. Lin, J. R.; Chen, L. W. *J. Appl. Polym. Sci.* **1998**, *69*, 1563.
12. Liu, H.; Li, S. C.; Liu, Y.; Iqbal, M. *J. Appl. Polym. Sci.* **2011**, *122*, 2512.
13. Lendlein, A.; Kelch, S. *Angew. Chem. Int. Ed.* **2002**, *41*, 2034.
14. Gunes, I. S.; Jana, S. C. *J. Nanosci. Nanotechnol.* **2008**, *8*, 1616.
15. Ratna, D.; Karger-Kocsis, J. *J. Mater. Sci.* **2008**, *43*, 254.
16. Leng, J. S.; Lan, X.; Liu, Y. J.; Du, S. Y. *Smart Mater. Struct.* **2009**, *18*, 1.
17. Luo, H. S.; Hu, J. L.; Zhu, Y. *Mater. Lett.* **2011**, *65*, 3583.
18. Auad, M. L.; Contos, V. S.; Nutt, S.; Aranguren, M. I.; Marcovich, N. E. *Polym. Int.* **2008**, *57*, 651.
19. Hearon, K.; Smith, S. E.; Maher, C. A.; Wilson, T. S.; Maitland, D. *J. Radiat. Phys. Chem.* **2013**, *83*, 111.
20. Dakin, V. *Radiat. Phys. Chem.* **1995**, *45*, 715.
21. Khonakdar, H. A.; Jafari, S. H.; Rasouli, S.; Morshedian, J.; Abedini, H. *Macromol. Theory Simulat.* **2007**, *16*, 43.